Available online at www.sciencedirect.com
ScienceDirect
Trans. Nonferrous Met. Soc. China 24(2014) 2168−2173
Transactions of Nonferrous Metals Society of China
www.tnmsc.cn

Simulation of temperature and stress in 6061 aluminum alloy during online quenching process

Meng-jun WANG[1,2], Gang YANG, Chang-qing HUANG[2], Bin CHEN[1]

1. Key Laboratory of Nonferrous Metal Materials Science and Engineering of Ministry of Education, Central South University, Changsha 410083, China;
2. State Key Laboratory of High-performance & Complicated Manufacturing, Central South University, Changsha 410083, China

Received 17 October 2013; accepted 17 April 2014

Abstract: The cooling curves of 6061 aluminum alloy were acquired through water quenching experiment. The heat transfer coefficient was accurately calculated based on the cooling curves and the law of cooling. The online quenching process of complex cross-section profile was dynamically simulated by the ABAQUS software. The results suggest that the heat transfer coefficient changes during online quenching process. Different parts of the profile have different cooling velocity, and it was verified by water quenching experiment. The maximum residual stress of the profile was predicted using FEM simulation based on ABAQUS software. The relations between the temperature and stress were presented by analyzing the data of key points.
Key words: 6061 aluminum alloy; quenching; complex cross-section profile; residual stress; ABAQUS

1 Introduction

6061 aluminum alloy is widely used in the production of large scale complex cross-sections architecture profiles and industrial profiles due to its characteristics of moderate intensity, nice plasticity, favorable solderability and corrosion resistance [1,2]. The complex cross-section profile has a wide range of application in the aerospace, train and hull structure. As for variations in thickness, shape (especially asymmetric structure) and the inability to cool inside the hollow section, there is non-uniform cooling both across the section and along the length of the section during the online quenching process [3,4]. This non-uniform cooling may lead to large temperature gradients, and cause high residual stresses and thermally induce distortions, such as warping and twisting [5−8]. This may severely affect the property and the precision of the products, and reduce the production. Therefore, it is very necessary to investigate the residual stresses of 6061 alloy parts after quenching. In order to predict the temperature and stress distributions of the complex cross-section profile in the online quenching process, ABAQUS/standard was applied to simulate the performance of the profile [9−11]. YANG et al [12] simulated the temperature field and residual stress of large complicated thin-wall workpieces by finite element method. LI et al [13] studied the temperature and stress fields of Ti-alloy thin-well barrel during quenching process. The heat transfer coefficient (HTC) is an important factor for quenching process, so it must be taken into account [14−16].

In this work, the study combining FEM with experimental methods was performed to analyze the temperature and stress distributions of a circular pipe of 6061 aluminum alloy. The cooling curves of 6061 aluminum alloy were obtained in water quenching. Based on the cooling curves, the HTC curves were solved. The temperature and stress distributions of a circular pipe of 6061 aluminum alloy were simulated by ABAQUS software, and the basis for preferable quenching techniques was offered.

2 Experimental

2.1 Quench experiment

6061 aluminum alloy was used for quenching

Foundation item: Project (zzyjkt2013-10B) supported by the Foundation of State Key Laboratory of High-performance & Complicated Manufacturing, China; Project (51275533) supported by the National Natural Science Foundation of China
Corresponding author: Meng-jun WANG; Tel: +86-731-88836408; E-mail: 347468230@qq.com
DOI: 10.1016/S1003-6326(14)63328-8

experiment to acquire heat transfer coefficient. Table 1 lists its chemical compositions. The shape and size of sample are shown in Fig. 1. Holes *A* and *B* were installed with thermocouple to get temperatures in the quenching process. Recycling water of 25 °C was used as quenchant. Figure 2 shows the corresponding cooling curves of Points *A* and *B*.

Table 1 Chemical compositions of tested 6061 aluminum alloy (mass fraction, %)

Si	Mg	Fe	Cu	Mn
0.62−0.67	0.95−1.00	≤0.35	0.17−0.21	0.10−0.15
Cr	Zn	Ti	Al	
0.05−0.10	≤0.05	0.02−0.05	Bal.	

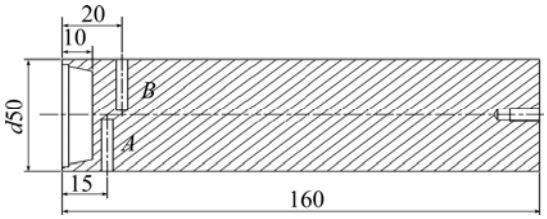

Fig. 1 Schematic diagram of quenching sample (unit: mm)

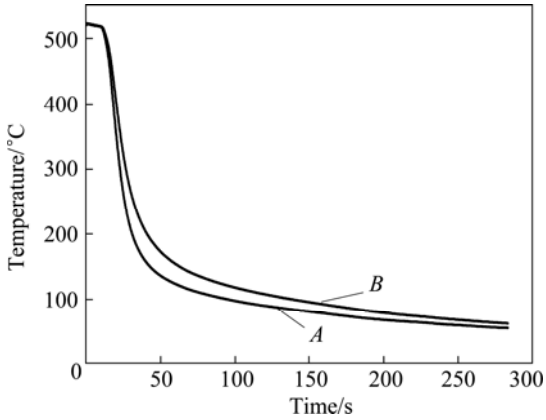

Fig. 2 Cooling curves of 6061 aluminum alloy in water quenching

2.2 Calculation of HTC

Precise HTCs are the key boundary conditions in simulating the quenching process, which was acquired from the past research results [17].

The quenching sample fits one-dimensional heat transfer model. Based on one-dimensional unsteady heat conduction differential equation, the temperature of the quenching surface can be defined as follows:

$$T_0(t)=2T_1(t)-T_2(t)+\frac{C_p\rho(\Delta x)^2}{\lambda\Delta t}[T_1(t+\Delta t)-T_1(t)] \quad (1)$$

where $T_0(t)$, $T_1(t)$ and $T_2(t)$ are the temperatures of quenching surface, the Points *A* and *B*, respectively; $T_1(t+\Delta t)$ refers to the temperature of Point *A* at moment $t+\Delta t$; λ, ρ, C_p are the thermal conductively, the mass density and the specific heat capacity, respectively; Δt and Δx refer to the temperature and displacement change amount.

Based on the Fourier law and Newton's law of cooling, the relationship between the quenching time *t*, face temperature $T_0(t)$ and HTC $h_w(t)$ can be described as

$$h_w(t)=\frac{q}{T_s-T_w}=\lambda\frac{T_1(t)-T_0(t)}{\Delta x[T_0(t)-T_w]} \quad (2)$$

where T_s is the temperature before quenching; T_w is the temperature of quenchant; q is the internal heat source density. According to the cooling curves, together with Eqs. (1) and (2), h_w-T_0 curve can be got, as shown in Fig. 3.

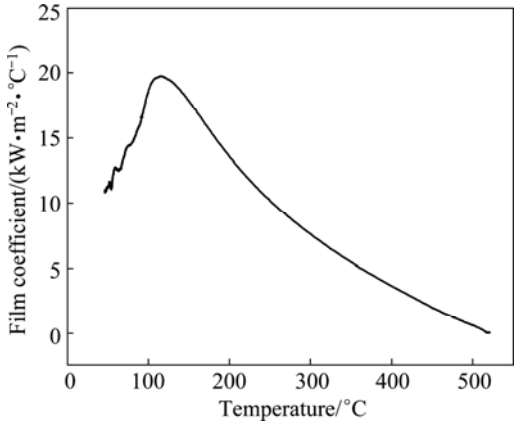

Fig. 3 HTC curves of 6061 aluminum alloy in quenching surface

2.3 Numerical simulation

ABAQUS/standard with coupled thermal displacement analysis was applied to simulate the quenching process. Since the cooling along the length axis was uniform, a 2D model was used to reduce the computational time. The scale of the model was in agreement with the real profile, as shown in Fig. 4. The physical properties of the alloy were considered to be constant in the models and listed in Table 2. The yield stresses at different temperatures are listed in Table 3 [18]. Element type was CPE4T and mesh size was properly selected. Reference Points *A*−*H* were also defined to extract data for analyzing the process.

3 Results and discussion

3.1 Temperature distribution

The temperature distributions in the quenching process at different time are shown in Fig. 5, from which, the maximum cooling velocity occurs in external edge of four ribs around the profile, while the joints of the internal face and ribs have the slowest cooling velocity.

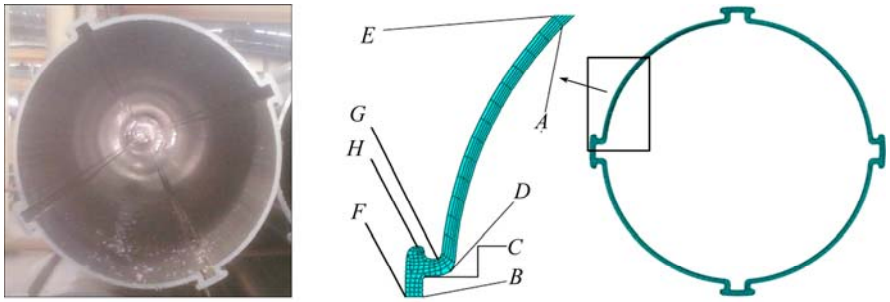

Fig. 4 Profile (a) and its FEM model (b)

Table 2 Material parameters of 6061 aluminum alloy

Conductivity/ ($W \cdot m^{-1} \cdot K^{-1}$)	Density/ ($g \cdot cm^{-3}$)	Specific heat capacity/ ($J \cdot kg^{-1} \cdot K^{-1}$)	Expansion coefficient	Elastic modulus/GPa	Poisson ratio
180	2.7	896	10^{-5}	40	0.35

Table 3 Yield stresses of 6061 aluminum alloy at different temperatures

Temperature/°C	24	100	150	200	260	316	371
Yield stress/MPa	276	262	214	105	34	19	12

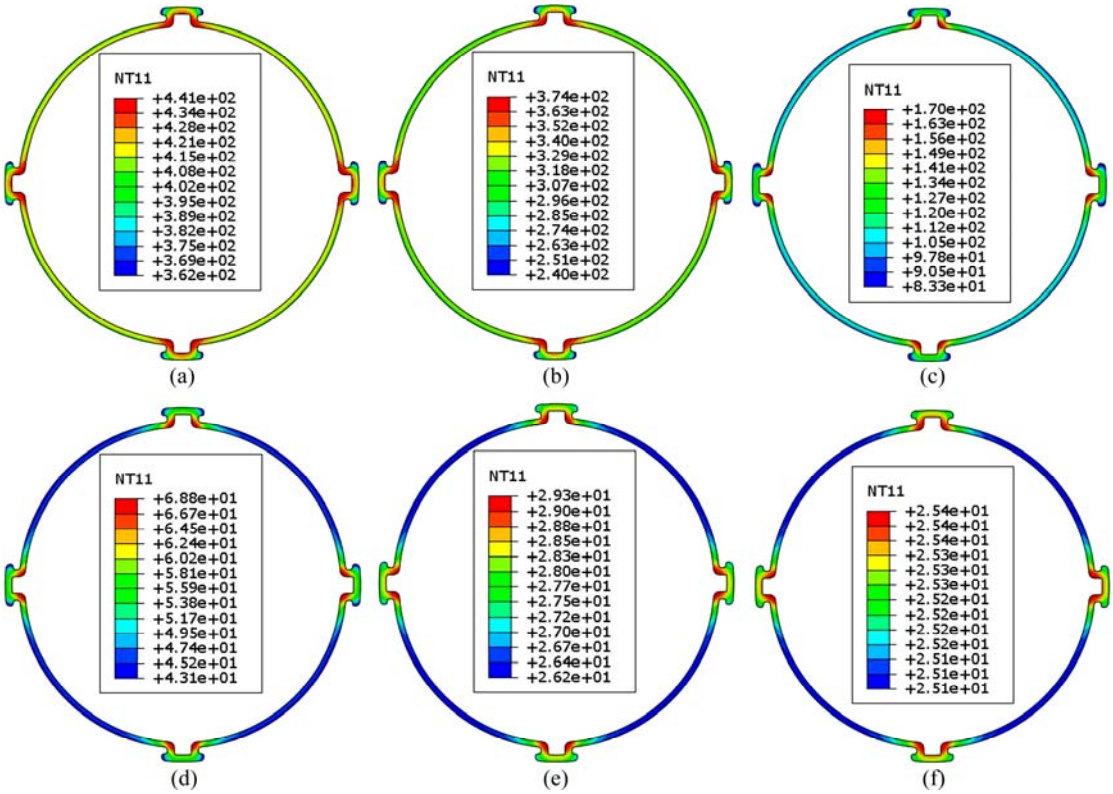

Fig. 5 Temperature distributions of profile model during quenching process at different time: (a) 0.5 s; (b) 1 s; (c) 2 s; (d) 3 s; (e) 5 s; (f) 7 s

As the temperature difference between the quenching medium and profile increases, the heat exchanges rapidly and the temperature drops sharply. The temperature difference of the profile maintains 100 °C in the first 2 s and then decreases apparently. Finally, the temperature of the entire profile tends to be uniform. As large temperature difference is prone to form residual stress, the heat induced stresses will concentrate in the rib, and the peak value appears within 2 s.

Figure 6 shows the cooling curves of key Points *A*−*H* of 6061 aluminum alloy profile at the water flow of 0.32 m^3/h. Among the internal points *A*−*D*, the maximum

cooling velocity appears in Points *A* and *D*, and the cooling velocity of Point *C* is smaller than that of the other three points. However, among the external Points *E*−*G*, Point *G* has the maximum cooling velocity, and point *H* has the smallest cooling velocity. It fits well with the cooling law which reflects in the temperature distributions of the profile model, as shown in Fig. 5.

3.2 Stress distribution

The stress distributions of the profile in different quenching time are shown in Fig. 7. At the beginning, the external walls of the pipe and ribs suffer tensile stress, however, the internal walls are under compressive stress, those stresses reverse as the temperature decreases. From the stress contours, it can be seen that stress concentration appears mainly in the joints of the pipe wall and ribs. The maximum residual stress exists around the joints of internal wall and ribs when the quenching process is over.

To further illustrate the relations between the temperature and the stress of the profile during the quenching process, data of the key Points *A*−*H* are

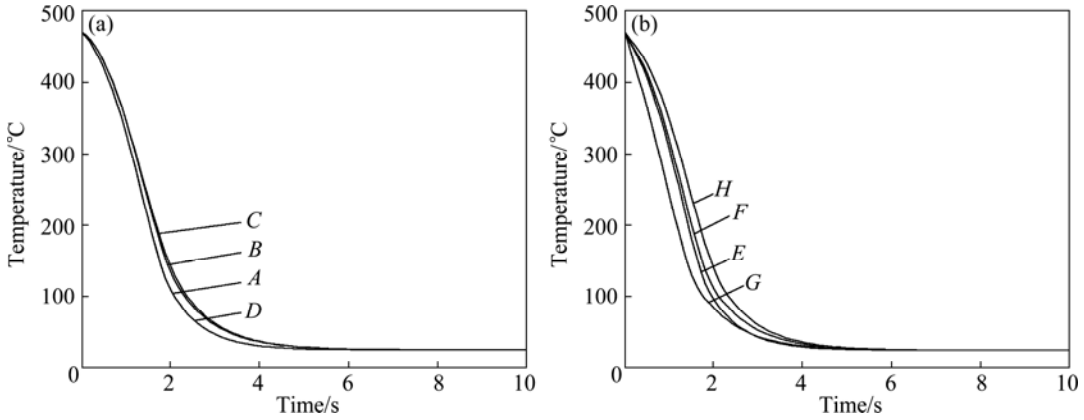

Fig. 6 Cooling curves of key Points *A*−*H* of 6061 aluminum alloy profile: (a) Internal Points *A*−*D*; (b) External Points *E*−*G*

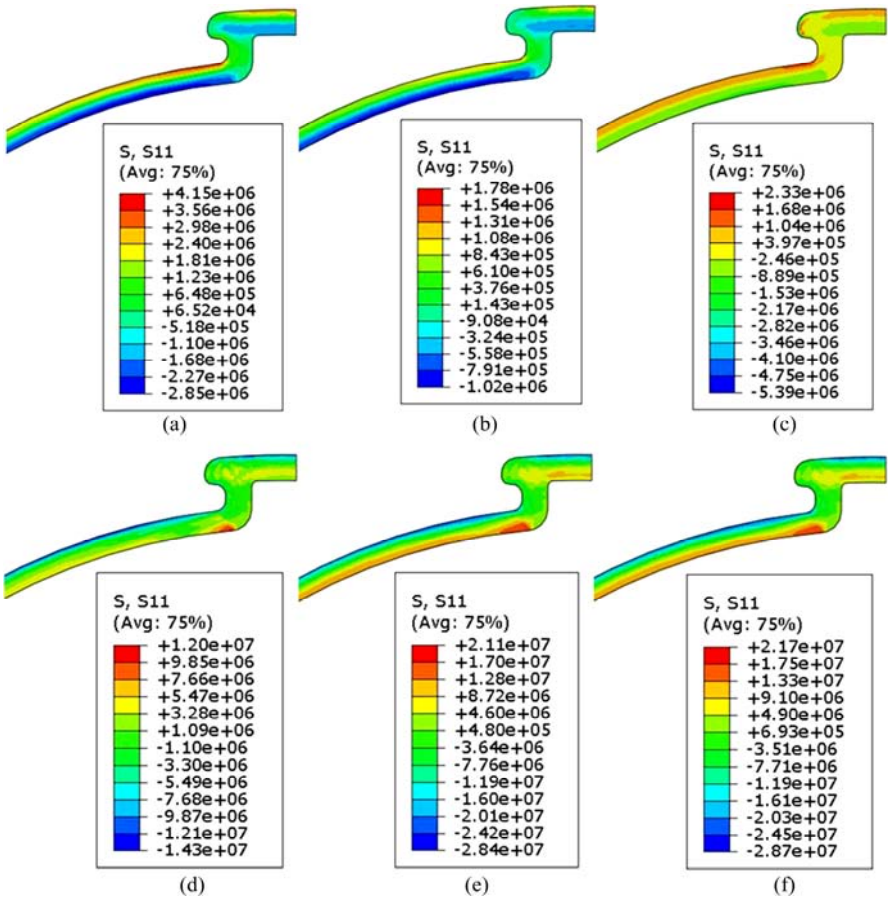

Fig. 7 Stress distributions of profile model during quenching process at different time: (a) 0.1 s; (b) 0.5 s; (c) 1 s; (d) 2 s; (e) 4 s; (f) 6 s

extracted. The temperature−stress curves are shown in Fig. 8. Points *A*−*D* suffer compressive stress firstly and then change to tensile stress. Finally, residual tensile stresses exist after quenching. Points *A*−*D* get to the peak compressive stress before 500 °C. When Points *B* and *C* get to the peak stress value, the corresponding temperature is even higher than that of Points *A* and *D*, while the peak stress values of Points *A* and *D* are larger than that of Points *B* and *C*. The peak compressive stresses of Points *A* and *D* in the initial stage are 1.5 and 1.3 MPa, respectively. And the residual tensile stresses after quenching are 8.2 and 7.7 MPa, respectively. On the contrary, stress states of Points *E*−*H* are tensile firstly, then change to compressive stress. In the first place, Points *E* and *G* reach the peak stress values of 1.7 and 2.8 MPa, respectively. Finally, residual compressive stresses reach 17.4 and 21.7 MPa, respectively.

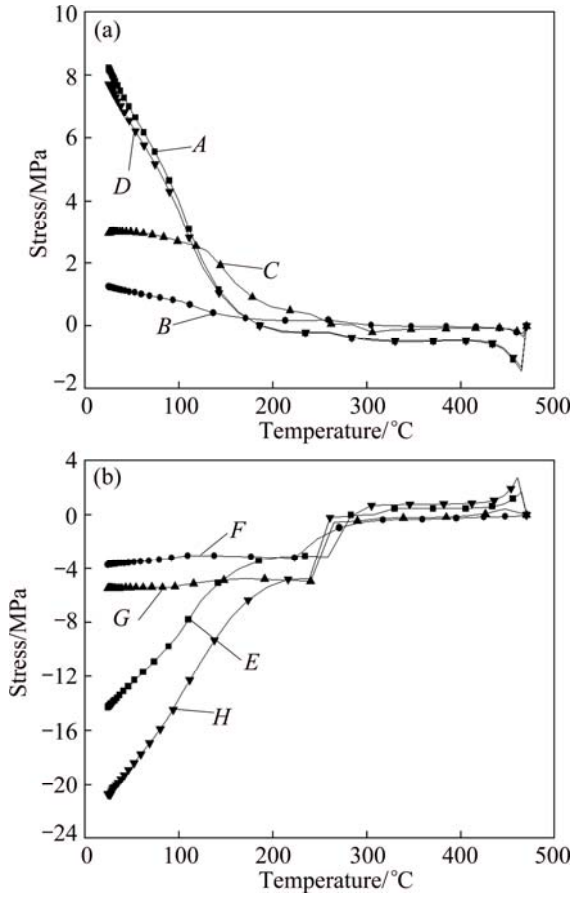

Fig. 8 Temperature−stress curves of key points during quenching process: (a) Internal Points *A*−*D*; (b) External Points *E*−*G*

4 Conclusions

1) The value of heat transfer coefficient is low at the beginning of the quenching process, however, with the temperature decreasing, it rises till the peak of 20 kW/(m^2·K) and then decreases.

2) The maximum cooling velocity appears in the external edge of ribs around the profile, while the joints of the internal surface and ribs have the slowest cooling velocity. The temperature difference of the profile is about 100 °C in the first 2 s, then decreases apparently. And the temperature of entire profile tends to be uniform. The cooling curves of key points fit well with the cooling law which reflects in the temperature distributions of the profile model.

3) The external walls of the pipe and ribs suffer tensile stress firstly, while the internal walls are under compressive stress, with the temperature decreasing, the stresses reverse. The maximal residual compressive stress and tensile stress in the quenching process are 28.7 and 21.7 MPa, respectively.

References

[1] JI Yan-li, GUO Fu-an, PAN Yan-feng. Microstructural characteristics and paint-bake response of Al−Mg−Si−Cu alloy [J]. Transactions of Nonferrous Metals Society of China, 2008, 18(1): 126−131.

[2] PAN Dao-zhao, WANG Zhi-xiu, Li Hai, ZHENG Zi-qiao. Effects of two-step ageing treatment on tensile properties and intergranular corrosion of 6061 aluminum alloy [J]. The Chinese Journal of Nonferrous Metal, 2010, 20(3): 435−441. (in Chinese)

[3] SHANG Bao-chuan, YIN Zhi-min, WANG Gang, LIU Bo. Investigation of quenching sensitivity and transformation kinetics during isothermal treatment in 6082 aluminum alloy [J]. Materials and Design, 2011, 32(7): 3818−3822.

[4] BIKASS S, ANDERSON B, PILIPENKO A, LANGTANGEN H P. Simulation of the distortion mechanisms due to non-uniform cooling in the aluminum extrusion process [J]. International Journal of Thermal Sciences, 2012, 52(1): 50−58.

[5] LI Hong-ying, ZENG Cui-ting, HAN Mao-sheng, LIU Jiao-jiao, LU Xiao-chao. Time−temperature−property curves for quench sensitivity of 6063 aluminum alloy [J]. Transactions of Nonferrous Metals Society of China, 2013, 23(1): 38−45.

[6] RUUD C O. Residual stresses and their measurement, quenching and distortion control [C]//Proceedings of the First International Conference on Quenching and Control of Distortion. Chicago: ASM International, 1992: 193−198.

[7] SARMIENTO G S, CASTRO M, TOTTEN G E, HARVIS L, WEBSTER G., CABR M F. Modeling residual stresses in spring steel quenching [J]. Heat Treatment of Metals, 2003, 28(11): 47−52.

[8] TANNER D A, ROBINSON J S. Residual stress prediction and determination in 7010 aluminum alloy forgings [J]. Experimental Mechanics, 2000, 40(1): 75−82.

[9] ZHANG Qing-feng, JIAO Si-hai, MA Zhao-hui. FEM simulation of temperature field in plate during quenching process [J]. Material and Heat Treatment, 2010, 39(6): 157−160. (in Chinese)

[10] XIAO B W, WANG Q G, PARAG J, LI K Y. An experimental study of heat transfer in aluminum castings during water quenching [J]. Journal of Materials Processing Technology, 2010, 210(1): 2023−2028.

[11] LI H P, ZHAO G Q, NIU S T, HUANG C Z. FEM simulation of quenching process and experimental verification of simulation results [J]. Material Science and Engineering A, 2007, 452−453: 705−714.

[12] YANG Xia-wei, ZHU Jing-chuan, LAI Zhong-hong, LIU Yong, HE Dong, NONG Zhi-sheng. Finite element analysis of quenching

temperature field, residual stress and distortion in A357 aluminum alloy large complicated thin-wall workpieces [J]. Transactions of Nonferrous Metals Society of China, 2013, 23(6): 1751−1760.

[13] LI Yan-zeng, YAN Mu-fu, WU Kun. Numerical simulation of temperature and stress fields of Ti-alloy thin-well barrel during quenching process [J]. Transactions of Meterials Heat Treatment, 2004, 25(5): 769−772.

[14] SHI Zhi-yu. Online quenching process practice of industrial aluminum [J]. Metallurgical Collections, 2010, 185(1): 43−45.

[15] CHEN Nai-lu, GAO Chang-yin, SHAN Jin, PAN Jian-sheng, YE Jian-song, LIAO Bo. Research on the cooling characteristic and heat transfer coefficient of dynamic quenchant [J]. Transactions of Materials and Heat Treatment, 2001, 22(3): 41−44.

[16] LI H P, ZHAO G Q, NIU S T. Technological parameters evaluation of gas quenching based on the finite element method [J]. Computational Materials Science, 2007, 40(2): 282−291.

[17] CHEN Bin, WEN Liu, PAN Xue-zhu, WANG Yin-xin, GAO Meng, WANG Meng-jun. The experiment research and simulation analysis on the online quenching process of the 6061 aluminum alloy [J]. Aluminum Fabrication, 2011, 5(1): 18−21. (in Chinese)

[18] WANG Zhu-tang, TIAN Rong-zhang. Handbook of aluminum alloy and processing [M]. Changsha: Central South University of Technology Press, 1988: 1015−1017. (in Chinese)

6061 铝合金在线淬火温度场和应力场模拟

王孟君[1,2]，杨 刚[1]，黄长清[2]，陈 彬[1]

1. 中南大学 有色金属材料科学与工程教育部重点实验室，长沙 410083；
2. 中南大学 高性能复杂制造国家重点实验室，长沙 410083

摘 要：通过淬火实验获得 6061 铝合金的冷却曲线，实验根据冷却曲线并结合数值方法获得在线淬火换热系数，运用 ABAQUS 有限元软件动态模拟复杂截面型材在线淬火过程。结果表明：在淬火过程中，换热系数不断变化；型材不同部位冷却速度不同，并通过淬火实验加以验证。通过 ABAQUS 有限元软件可以预测型材的最大残余应力；通过关键点的分析得出型材温度与应力的关系曲线。

关键词：6061 铝合金；淬火；复杂截面型材；应力；ABAQUS

(Edited by Chao WANG)